論文 / 著書情報
Article / Book Information

Title	A performance model for the communication in fast multipole methods on high-performance computing platforms
Author	Huda Ibeid, Rio Yokota, David Keyes
Journal/Book name	International Journal of High Performance Computing Applications, Vol. 30, No. 4, pp. 423--437
Issue date	2016, 3
DOI	http://dx.doi.org/10.1177/1094342016634819
Note	このファイルは著者（最終）版です。 This file is author (final) version.

A Performance Model for the Communication in Fast Multipole Methods on HPC Platforms

Huda Ibeid, Rio Yokota, and David Keyes
Division of Computer, Electrical and Mathematical Sciences and Engineering
King Abdullah University of Science and Technology, Saudi Arabia

Abstract

Exascale systems are predicted to have approximately one billion cores, assuming Gigahertz cores. Limitations on affordable network topologies for distributed memory systems of such massive scale bring new challenges to the currently dominant parallel programing model. Currently, there are many efforts to evaluate the hardware and software bottlenecks of exascale designs. It is therefore of interest to model application performance and to understand what changes need to be made to ensure extrapolated scalability. The fast multipole method (FMM) was originally developed for accelerating N-body problems in astrophysics and molecular dynamics, but has recently been extended to a wider range of problems, including preconditioners for sparse linear solvers [31]. Its high arithmetic intensity combined with its linear complexity and asynchronous communication patterns make it a promising algorithm for exascale systems. In this paper, we discuss the challenges for FMM on current parallel computers and future exascale architectures, with a focus on inter-node communication. We focus on the communication part only; the efficiency of the computational kernels are beyond the scope of the present study but see, e.g., [3]. We develop a performance model that considers the communication patterns of the FMM, and observe a good match between our model and the actual communication time on four HPC systems, when latency, bandwidth, network topology, and multi-core penalties are all taken into account. To our knowledge, this is the first formal characterization of inter-node communication in FMM that validates the model against actual measurements of communication time. The ultimate communication model is predictive in an absolute sense; however, on complex systems, this objective is often out of reach, or of a difficulty out of proportion to its benefit when there exists a simpler model that is inexpensive and sufficient to guide coding decisions leading to improved scaling. The current model provides such guidance.

1 Introduction

N-body problems arise in many areas of physics (e.g., astrophysics, molecular dynamics, acoustics, electrostatics). In these problems, the system is described by a set of N particles and the dynamics of the system arise from interactions that occur between every pair of particles. This requires $\mathcal{O}(N^2)$ computational complexity. For this reason, many efforts have been directed at producing *fast* N-body algorithms. More efficient algorithms of the particle interaction problem can be provided by a hierarchical approach using tree structures. In this approach, the computational domain is hierarchically subdivided, and the particles are clustered into a hierarchical tree structure. An approximation of tunable accuracy is applied to far-field interactions, whereas near-field interactions are summed directly. When the far-field expansion is calculated against the particles directly, this approach called a treecode [1]. When the far-field effect is translated to local-expansions before summing their effect, it is called a fast multipole method (FMM) [15, 5]. These approaches bring the complexity down to $\mathcal{O}(N \log N)$ and $\mathcal{O}(N)$ for treecode and FMM, respectively. FMM has been listed as one of the top ten algorithms of the twentieth century [8] due to its wide applicability and impact on scientific computing. It was originally developed for applications in electrostatics and astrophysics, but continues to find new areas of application such as aeroacoustics [29], fluid dynamics [14], magnetostatics [28], and electrodynamics [33]. Because of its linear complexity, FMM scales well with respect to the problem size, if implemented efficiently. For future computer systems the conservation of flops is less important than the conservation of distant loads and stores to supply the

arguments for the flops. FMM stands out among hierarchical O(N) algorithms for its strong arithmetic intensity.

Since the performance of a single-processor core has plateaued, future supercomputing performance will depend mainly on increases in system scale rather than improvements in single-processor performance. Processor counts are already in the millions for the top system. Modeling application performance at such scales is required to guide algorithmic choices and tunings on existing architectures and evaluate contemplated architectures. Since the performance of the FMM has a large impact on a wide variety of applications across a wide range of disciplines, it is important to understand the challenges that FMM implementations face on architectures with increased parallelism, as well as to predict and locate bottlenecks that might cause performance degradation. On future architectures where computation becomes relatively cheap compared to data movement, we anticipate that inter-node communication will become the bottleneck. The priority of the present study is the communication model of FMM.

To model the performance, we start with the baseline model, namely (α, β) model for communication, where α is the latency and β is the inverse bandwidth. Then, some penalties are added to the baseline model based on machine constraints. These penalties include distance and reduced per-core bandwidth. Our performance model is related to universal communication features and can be applied regardless of local FMM implementation choices, core-scale machine characteristics that do not affect communication, and arithmetic workload associated with other aspects of the computation. Of course, the importance of communication as a bottleneck depends strongly on the cost of other tasks, but it is important to be able to evaluate communication costs as a component in an overall cost model. The Byte-count parameters in our model makes it adaptable to any of the various FMM implementations, while the penalties in our model are tunable to various architectures. We validate our performance model on four different architectures, Shaheen (BG/P), Mira (BG/Q), Titan (Cray XK7), and Piz Dora (Cray XC40).

The focus of this paper is on characterizing the FMM communication, not on introducing a new model. For this purpose, we apply a performance model developed originally and applied to multigrid methods, which have a different communication pattern. A new application of an existing tool emphasizes the versatility of the tool. Meanwhile, such detailed analysis of the communication in FMM has not previously been reported, so there is particular relevance to the FMM community, and to the HPC community that exploits, or will exploit at exascale, FMM solvers.

The paper is organized as follows. Section 2 gives an overview of related work. Section 3 summarizes some performance challenges that face FMM on parallel machines. These challenges include massive parallelism and degradation due to inter-node communication. In Section 4, an exposition of the fast multipole method sufficiently detailed to expose communication properties is given. Section 5 describes our performance model. Experiments done to validate the performance models are provided in Section 6 and we conclude in Section 8.

2 Related work

Performance modeling and characterization for understanding and predicting the performance of scientific applications on HPC platforms have been targeted by many related projects. For example, Clement and Quinn developed a performance prediction methodology through symbolic analysis of their source code [6]. Mendes and Reed focused on predicting scalability of an application program executing on a given parallel system [24]. Mendes proposed methodology to predict the performance scalability of data parallel applications on multi-computers based on information collected at compile time [23]. The approach of combining computation and communication to obtain a general performance model is described by Snavely *et al.* [27]. DeRose and Reed concentrate on tool development for performance analysis [7]. Performance models for implicit CFD codes have been considered [17]. The efficiency of the spectral transform method on parallel computers has been evaluated by Foster [10]. Kerbyson *et al.* provide an analytical model for the application SAGE [19]. Performance models for AMG were developed by Gahvari *et al.* [11], who have also analysed the performance of AMG over a dragonfly network in [12]. Traditional evaluation of specific machines via benchmarking is presented by Worley [30].

Scaling FMM to higher and higher processor counts has been a popular topic [25, 18], while extensive study of single-node performance optimization, tuning, and analysis of FMM has also been of interest [4]. However, there has been little effort to model the inter-node communication of FMMs. Lashuk *et al.* derive the overall complexity of FMM on distributed memory heterogeneous architectures [20], but do not validate the model against the actual performance. The present work is based on the communication

model for AMG [11], and extends their theory to FMM. To our knowledge, this is the first formal characterization of inter-node communication in FMM, which validates the model against actual measurements of communication time.

3 Performance challenges

High performance computing systems have shown a sustained exponential growth with performance improvement of approximately 10x every 3.6 years as measured, for instance, by the Gordon Bell Prizes or the Top500 benchmark over the past 2.5 decades. This performance improvement comes at a cost in code complexity and introduces many challenges. Furthermore, the development of an exascale computing capability will cause significant and dramatic changes in computing hardware architecture relative to current petascale computers. In this section we present some of the challenges faced by FMMs to achieve good parallel performance on future exascale systems.

3.1 Trends in Computer Hardware

Computers consisting of nodes in the tens of thousands with cores per node in the hundreds have emerged as the most widely used high-performance computing platforms. These nodes communicate by sending messages through a network, which leads to lower scalability and less performance due to cores on a single node contenting for access to the interconnect. We discuss multicore and manycore issues in more detail when presenting our performance models that take this into account.

3.2 Communication

Two types of costs in terms of time and energy are usually analyzed separately: computation (flops) and communication (Bytes). Communication involves moving data between levels of a memory hierarchy in case of sequential algorithms and exchanging data between processors over a network in the case of parallel algorithms. Therefore, without considering overlap, the running time of an algorithm is the sum of three terms: the number of flops times the time per flop, the number of words moved divided by the bandwidth (measured as words per unit time), and the number of messages times the latency. The last two terms determine the time consumed by communication. The time per flop is already an order of magnitude less than reciprocal bandwidth and latency and the gaps between computation and communication are growing exponentially with time. (See Table 2 under the machine descriptions in Section 6 below.) Communication performance models can guide development of algorithms to help reduce the communication.

4 Fast multipole method

N-body methods are most commonly used to simulate the interaction of particles in a potential field, which has the form

$$f(\mathbf{x}_i) = \sum_{j=1}^{N} q_j K(\mathbf{x}_i, \mathbf{x}_j) \tag{1}$$

Here, $f(\mathbf{x}_i)$ represents a field value evaluated at a point $\mathbf{x}_i$ which is generated by the influence of sources located at $\mathbf{x}_j$ with weights q_j. $K(\mathbf{x}_i, \mathbf{x}_j)$ is the kernel that governs the interactions between evaluation and source particles. The direct approach to simulate the N-body problem is relatively simple; it evaluates all pair-wise interactions among the particles. While this method is exact to within machine precision, the solution is $\mathcal{O}(N^2)$ in its computational complexity, which is prohibitively expensive for even modestly large data sets. However, its simplicity and ease of implementation make it an appropriate choice when simulating small particle sets ($N < 1000$) where high accuracy is desired [26]. For a larger number of particles, many faster algorithms have been invented, e.g., treecodes [1] and, the fast multipole method (FMM) [15]. The main idea behind these fast algorithms is to coarse grain the effect of sufficiently far particles as permitted by rigorous analysis. The most common way to achieve this approximation is to cluster the far particles into successively larger groups by constructing a tree. The treecode clusters the far particles and achieves $\mathcal{O}(N \log N)$ complexity. The FMM further clusters the near particles in addition to the far particles to achieve $\mathcal{O}(N)$ complexity.

In this section, we present an overview of fast algorithms that have been developed for the calculation of N-body problems. First, the spatial hierarchy and the fast approximate evaluation of these algorithms are discussed. Then, a description of the communication introduced by the domain partitioning scheme used in these algorithms is provided. The main focus is on the data flow of the FMM algorithm for which we develop the performance model.

4.1 FMM Overview

This overview is intended to introduce some key ingredients of the FMM. The mathematics behind the

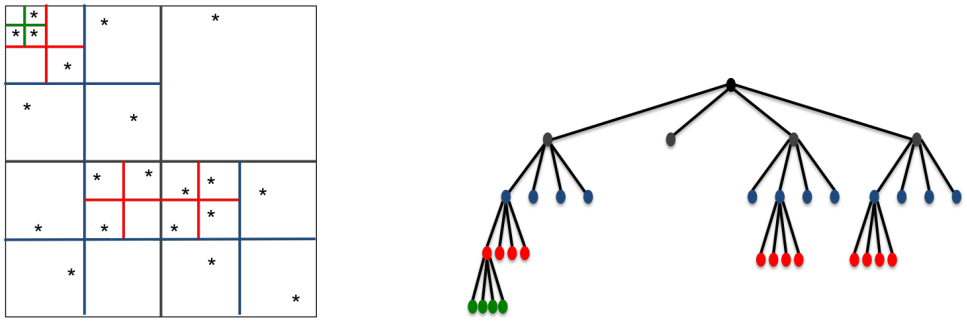

(a) 2-D view

(b) Tree view

Figure 1: Hierarchical decomposition

specific FMM kernels is well documented elsewhere and its detail conveniently decouples, given a simple interface to the communication model. For details of the mathematics we refer the reader to previous publications on FMM [2, 5].

4.1.1 Basic Component

Both treecodes [1] and the FMM [15] are based on two key ideas: the tree representation for the spatial hierarchy, and the fast approximate evaluation. The spatial hierarchy means that the computational domain is hierarchically decomposed into increasing levels of refinement, and then the near and far subdomains can be identified at each level. The three-dimensional spatial domain of the treecode and FMM is represented by octrees, where the space is recursively subdivided into eight cells until the finest level of refinement or "leaf level. Figure 1 illustrates such a hierarchical space decomposition for a two-dimensional domain (a), associated to a quad-tree structure (b). The original FMM [16] is based on a series expansion of the Laplace Green's function $(1/r)$ and therefore can be applied to the evaluation of related potentials and/or forces [13]. The approximation reduces the number of operations in exchange for accuracy.

4.1.2 Flow of Calculation

Figure 2, shows the flow of FMM where the effect of the source particles, shown in red in the lower left corner, are calculated on the target particles, shown in blue in the lower right corner. The schematic is a 2-D representation of what is actually a 3-D octree structure. The calculation starts by transforming the mass/charge of the source particles to a multipole expansion (P2M). Then, the multipole expansion is translated to the center of larger cells (M2M). Then, the influence of multipoles on the particles is calculated in three steps. First, it translates the multipole expansion to a local expansion (M2L). Next, the center of expansion is translated to smaller cells (L2L). Finally, the effect of the local expansion in the far field is translated onto the target particles (L2P). All pairs interaction is used to calculate the effect of near field on target particles (P2P).

4.2 FMM Communication Scheme

Partitioning of the FMM global tree structure and communication stencils is shown in Figure 3. The binary tree on the left side is a simplification of what is actually an octree in a 3-D FMM. Likewise, the schematics on the right are a 2-D representation of what is actually a 3-D grid structure. Each leaf of the global tree is a root of a local tree in a particular MPI process, where the global tree has L_{global} levels, and the local tree has L_{local} levels. Each process stores only the local tree, and communicates the halo region at each level of the local and global tree as shown in the red hatched region in the four illustrations on the right. The blue, green, and black lines indicate global cell boundaries, process boundaries, local cell boundaries, respectively. The switch between local and global trees produces a change in the communication pattern, as revealed in the heat map in Figure 4, where the switch is between levels 3 and 4.

5 Modeling Performance

Performance modeling is a key ingredient in high performance computing. It has a great importance in the design, development and optimization of applications, architectures and communication systems. It also plays a crucial role in understanding important performance bottlenecks of complex systems. For this reason, performance models are used to analyze, predict, and calibrate performance for systems of interest. The tree-based communication of FMM is in-

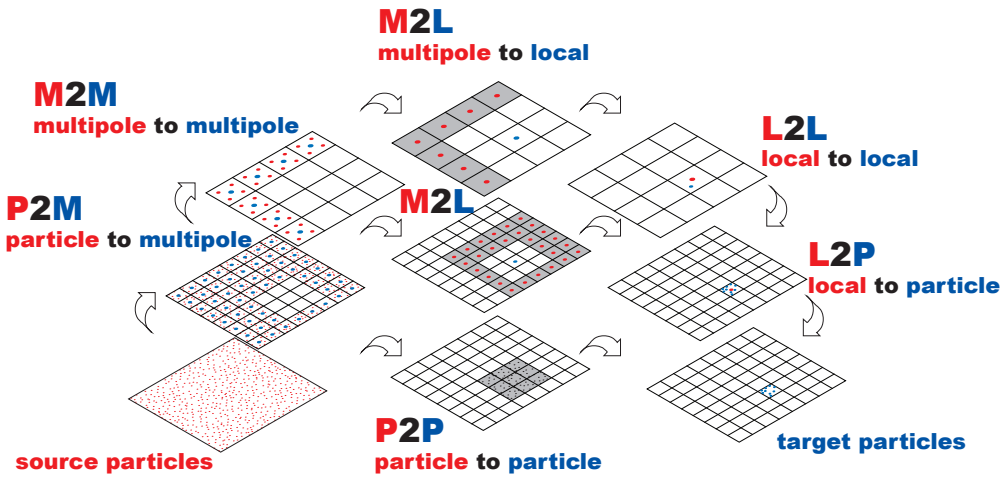

Figure 2: Data-flow of FMM calculation. Data dependency is between red and blue points.

.

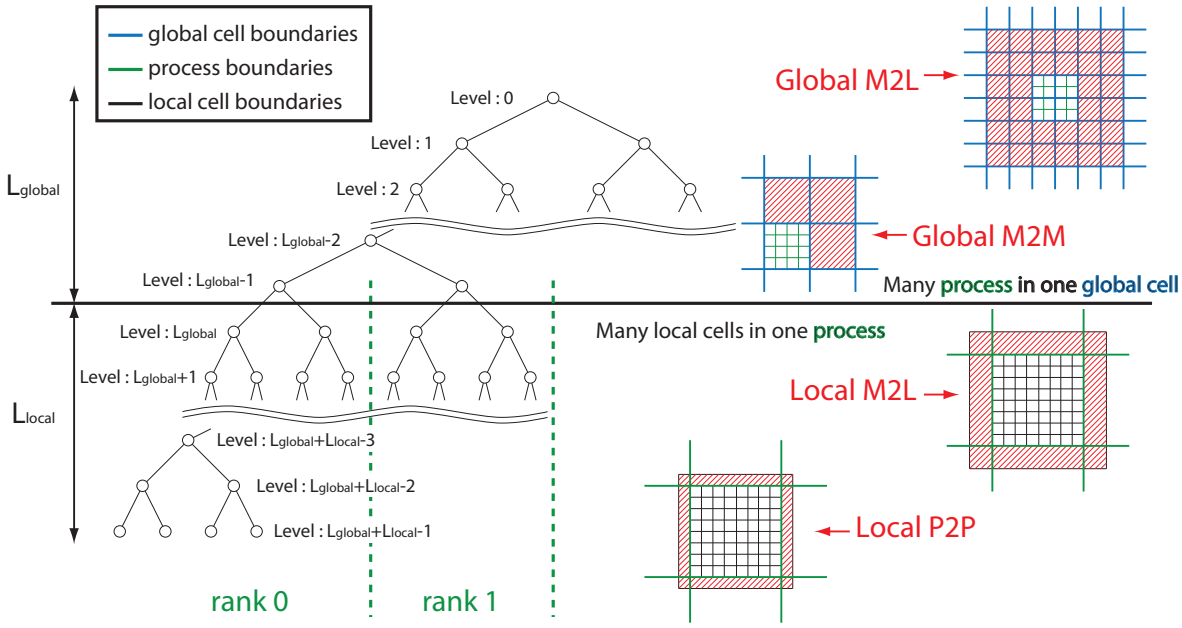

Figure 3: Splitting of the local and global tree in FMM.

creasingly important in HPC applications, both of FMM itself and, for instance, of hierarchically low-rank (or "rank-structured") matrices, which are under active development in theory and software. The application of a model of demonstrated relevance to one application to an entirely different application makes a statement about the value and general applicability of the model. In this section we develop a performance model to understand the performance of the communication in FMM through a phase-by-phase analysis based on four principal phases.

We start with a baseline model that is a combination of the latency and inverse bandwidth. We subsequently refine this baseline model to reach a more realistic model that is able to cover the relevant system architecture properties, with the exception that overlapping communication with computation is not considered in this work.

5.1 FMM Communication Phases

As shown in Figure 3, our FMM uses a separate tree structure for the local and global tree. In order to construct a performance model for the communication in

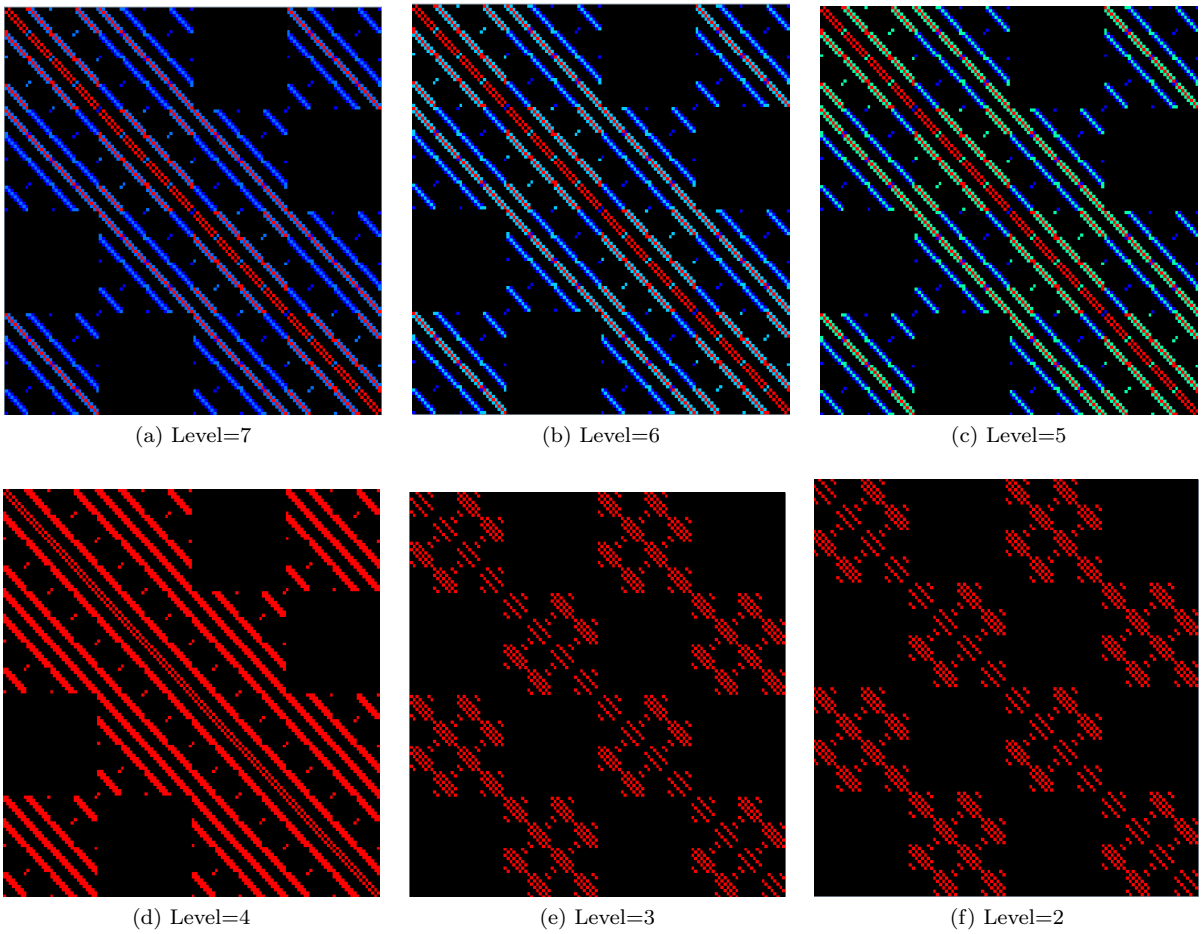

(a) Level=7 (b) Level=6 (c) Level=5

(d) Level=4 (e) Level=3 (f) Level=2

Figure 4: Heat maps for level-by-level communication patterns for the M2L phase of an FMM with N=62,500 per process using 128 processes. Areas of black indicate zero messages between processes, the peak communication volume is represented in red. In this example, the switch between global and local trees is between Level 3 and Level 4.

FMM, we estimate the amount of data that must be sent at each level of the hierarchy. Table 1 shows the number of cells that are sent, which correspond to the illustrations in Figure 3. L_{global} is the depth of the global tree, L_{local} is the depth of the local tree. We define N as the global number of particles, and P as the number of processes (MPI ranks). The global tree is constructed so that each MPI process is a leaf node in the global tree. Therefore, the depth of the global tree only depends on the number of processes P and not N. The depth of the global tree grows with $\log_8 P$, whereas the depth of the local tree grows with $\log_8(N/P)$. For the current calculations we are assuming a nearly uniform particle distribution (as in explicit solvent molecular dynamics) and therefore a full octree structure.

5.1.1 Global M2L

In Table 1 we show the number of cells to send per level and the total amount of communication for all levels. There are four types of communication in our FMM, which correspond to the four stages shown with the red hatching in Figure 3. The first is the "Global M2L" communication, which sends 26×8 cells at each level, as shown at the top right of Figure 3. The green lines are the process boundaries and the blue lines are the cell boundaries, which means one FMM cell belongs to many processes in the global tree. In order to avoid redundant communication, we index each process that shares a global cell and perform a one-to-one communication between the processes with matching indices only. In order to further reduce the communication, we select one process for a group of eight cells to do the communication. There-

fore, the number of processes to communicate with (p_i) is always 26 and the number of cells to send is always 8 for every process and for every level in the global tree. In other words, for the "Global M2L" communication the message size and number of sends is constant regardless of N and P, and only the number of hops between the processes will increase depending on the network topology. On torus networks, we map the MPI ranks to the torus and synchronize the direction of the 26 one-to-one communications. The communication per level is $\mathcal{O}(1)$ and the number of levels in the global tree is $\mathcal{O}(\log P)$, so the total communication complexity for this stage is $\mathcal{O}(\log P)$ as shown in Table 1.

5.1.2 Global M2M

The second type of communication is the "Global M2M", which sends 7 cells at each level, as shown in Figure 3. We use a similar technique to the "Global M2L" case to avoid redundant communication by pairing the MPI ranks for the one-to-one communication when many processes share the same global cell. The number of processes to communicate with is always seven and the number of cells to send is always one for every process and for every level in the global tree. Similar to the "Global M2L" case, only the number of hops during the one-to-one communication will increase, and the rate depends on the network topology. The communication per level is $\mathcal{O}(1)$ and the number of levels is $\mathcal{O}(\log P)$, so the total communication is $\mathcal{O}(\log P)$ for the "Global M2M" stage.

5.1.3 Local M2L

The third type of communication is the "Local M2L", which is shown in the red hatching in the second picture from the bottom on the right side of Figure 3. The process boundaries shown in green are coarser than the local cell boundaries shown in black, which means that one process contains many cells, in contrast to the previous two communication types. In a full octree structure, we know that all cells are non-empty so we simply need to send two layers of halo cells for the M2L calculation at each level, as shown in Figure 3. Therefore, the number of processes to communicate with is always the 26 neighbors, and the number of cells to send depends on the level. At level i of the local tree, there are 2^i cells in each direction. Two layers of halo cells on each size will create a volume of $(2^i+4)^3$ cells, and subtracting the center volume 8^i will give $(2^i+4)^3-8^i$ as shown in Table 1. The leading term is $\mathcal{O}(4^i)$ since the 8^i term cancels out. Since the number of levels in the local tree grow as $\log_8(N/P)$ the communication complexity for the "Local M2L" is $\mathcal{O}(4^{\log_8(N/P)}) = \mathcal{O}((N/P)^{2/3})$. This can also be understood as the surface to volume ratio of the bottom two illustrations in Figure 3. Since N/P is constant for weak scaling and decreases for strong scaling, this part does not affect the asymptotic weak/strong scalability of the FMM.

Table 1: Amount of communication in FMM

	Cells to send / level	Total comm.
Global M2L	26×8	$\mathcal{O}(\log P)$
Global M2M	7	$\mathcal{O}(\log P)$
Local M2L	$(2^i+4)^3-8^i$	$\mathcal{O}((N/P)^{2/3})$
Local P2P	$(2^i+2)^3-8^i$	$\mathcal{O}((N/P)^{2/3})$

5.1.4 Local P2P

The fourth type of communication in the FMM is the "Local P2P", which is shown in the bottom picture on the right side of Figure 3. This communication only happens at the bottom level of the local tree. Similar analysis to the "Local M2L" stage shows that $(2^i+2)^3-8^i$ cells must be sent, as shown in Table 1. In this case, i is exactly $\log_8(N/P)$ and we obtain the same asymptotic amount of communication of $\mathcal{O}((N/P)^{2/3})$. Similar to the "Local M2L", this part does not affect the asymptotic weak/strong scalability of the FMM. However, the content of the data is different from the previous three cases where the multipole expansion coefficients were being sent. In the P2P communication the coordinates and the charges of every particle that belongs to the cell must be sent. Therefore, the asymptotic constant of $\mathcal{O}(N/P)^{2/3}$ is typically much larger than that of the "Local M2L", and this could be the dominant part of the communication time depending on the number of particles per leaf cell.

5.2 Baseline Model ((α, β) model)

To model interprocess communication, we begin with the basic (α, β) model, where α represents communication latency, where β is the send time per-Byte (inverse bandwidth). Using the basic model, a message send cost can be represented as

$$T_{\alpha-\beta} = \alpha + n\beta \tag{2}$$

where n is the number of Bytes in the message.

This basic model describes the communication over an ideal architecture where the communication cost does not depend on processor locations or network traffic caused by many processors communicating at the same time [9]. For a more realistic architecture,

a more detailed model is needed. For this reason, we add penalties to this basic model to take into account machine-specific performance issues. In particular, we consider communication distance, interconnection switching delay, limited bandwidth, and the effect of multiple cores on a single node contending for available resources.

5.3 Distance Penalty ((α, β, γ) Model)

Following [11], we refine the assumption that distance between processors in interconnected networks does not have effect on communication time. To take into account the effect of distance we refine the baseline model according to the number of extra hops a message travels

$$T_{\alpha-\beta-\gamma} = \alpha + n\beta + (h - h_m)\gamma, \tag{3}$$

where h is the number of hops a message travels, h_m is the smallest possible number of hops a message can travel in the network, and γ is the delay per extra hop. If there is no network contention and all messages travel with minimum number of hops, this distance penalty should have no effect.

5.4 Bandwidth Penalty on β

The peak hardware bandwidth is rarely achieved in message passing. Therefore, we multiply β by B_{max}/B to incorporate the ratio between the peak hardware per-node bandwidth B_{max} and the effective bandwidth from the benchmark B.

$$T_{\beta-Penalty} = \alpha + n\beta\frac{B_{max}}{B} + (h - h_m)\gamma \tag{4}$$

5.5 Multicore Penalty on α or γ

Increasing the number of cores per node increases the data traffic between nodes, and could potentially result in congestion. Furthermore, larger number of cores per node introduces more noise caused by access to resources shared by multiple cores. To model these effects, we multiply α and/or γ by the number of active cores per node c. This model focuses on the worst case behavior where a machine's aggregate bandwidth could be exceeded by all cores communicating simultaneously. The resulting models are

$$T_{\alpha-Penalty} = c\alpha + n\beta + (h - h_m)\gamma \tag{5}$$
$$T_{\gamma-Penalty} = \alpha + n\beta + c(h - h_m)\gamma \tag{6}$$

6 Model Validation

6.1 Machine Description

To validate our performance models we benchmark our FMM code on four different architectures; Shaheen, Mira, Titan, and Piz Dora.

Shaheen is 16 racks of an IBM BlueGene/P. Each rack contains 1024 PowerPC 450 CPUs with 4 cores running at 850MHz with 32kB private L1 cache and 8MB shared L3 cache. Each compute node has 2GB RAM with 13.6 GB/s memory bandwidth. The nodes are connected by 3-D torus network with 5.1GB/s injection bandwidth per node.

Mira is 48 racks of an IBM BlueGene/Q. Each rack contains 1024 Power A2 CPUs with $16 + 1$ cores running at 1.6GHz with 16kB private L1 cache and 32MB shared L2 cache. Each compute node has 16GB RAM with 42.6GB/s memory bandwidth. The nodes are connected by a 5-D torus network with 20GB/s injection bandwidth per node.

Titan is a Cray XK7 system with $18,688$ compute nodes each equipped with an AMD Opteron 6274 CPU and NVIDIA Kepler K20X GPU. The CPU has 16 cores running at 2.2 GHz with 16 kB L1 cache, 2×4 MB L2 cache, and 8×2 MB L3 cache. The GPU has 15×64 cores running at 730 MHz with $64 + 48$ kB L1 cache and 1.5 MB L2 cache. Each compute node has 32 GB of RAM with 51.2 memory bandwidth. The nodes are connected by a 3-D torus with 20GB/s of injection bandwidth per node. We do not use any of the GPUs in the current study.

Piz Dora is a Cray XC40 with 1256 compute nodes, each with two 12-core Intel Haswell CPUs (Intel®Xeon®E5-2690 v3). Piz Dora has a total of 30144 cores (24 cores per node). Out of the total, 1192 nodes feature 64GB of RAM each, while the remaining 64 compute nodes have 128GB of RAM each (fat nodes). The nodes are connected by a dragonfly network using the Aries interconnect where the routers in each group are arranged as rows and columns of a rectangle, with all-to-all links across each row and column but not diagonally.

In order to obtain the machine parameters, the `b_eff` benchmark in the HPC Challenge suite [22] was used to determine the parameters α and β. We report the best-case latency and bandwidth measurements. To find the parameter γ, we followed the same procedure as Gahvari *et al.* [11]. The machine parameters for Shaheen, Mira, Titan, and Piz Dora are shown in Table 2. Note that our definition of β is defined as send time per Byte, whereas Gahvari *et al.* define their β as send time per element (8 Bytes).

Table 2: Machine parameters for latency α, inverse bandwidth β, and distance penalty γ, on Shaheen, Mira, Titan, and Piz Dora.

	Shaheen	Mira	Titan	Piz Dora
α	4.12 μs	5.33 μs	1.67 μs	0.457 μs
β	2.14 ns	1.32 ns	1.62 ns	0.4054 ns
γ	29.9 ns	134 ns	284 ns	0.4838 μs

6.2 Experimental Setup

We ran the FMM code for 10 steps and measured the time spent on the communication for the "Global M2L" and "Local M2L" phases. The results are then divided by 10 to get the average time spent at each level. The "Global M2M" phase was negligible and the "Local P2P" phase only occurs at the bottom level and is irrelevant to the scalability of the FMM, so we do not consider these two phases in the current analysis. We used the Laplace kernel in three dimensions with random distribution of particles in a cube. We use periodic boundary conditions so that there is no load imbalance at the edges of the domain. The number of MPI processes was varied between $P = \{128, 1024, 8192\}$, while the number of particles per process was kept constant at $N/P = 62,500$. On all machines we used the maximum number of cores on each node before increasing the number of nodes. Timings were measured with `gettimeofday()` after a `MPI_Barrier()` call. We used the default rank mapping to the nodes that the system provides.

Table 3 shows communication information and statistics when running the FMM on 128, 1024, and 8192 processes. "Level" is the level within the tree structure and goes from 0 to $L_{global}+L_{local}-1$, where $L_{local} = 4$ for $N/P = 62,500$. Therefore, the bottom four levels in Table 3 (a), (b), and (c) belong to the local tree. The depth of the global tree L_{global} is 4, 5, and 6 for 128, 1024, and 8192 processes, respectively. "Cells" is the total number of cells at that level of the tree structure, which is simply 8^{Level} for a full octree. "Sends" is the number of processes to which sends. As mentioned in Section 5.1 we have developed a communication scheme that limits the number of sends to 26 regardless of the problem size, number of processes, or the level. "Bytes" is the aggregate data size that is sent by a given process at each level of the tree. As shown in Table 1, the number of cells for the "Global M2L" communication is 26×8. For each cell we are sending 56 multipole expansion coefficients in single precision (4 Bytes). Therefore, the total number of Bytes for the "Global M2L" phase is $26 \times 8 \times 56 \times 4 = 46592$. We can see from Table 1 that the amount of cells involved in the "Local M2L" communication can be calculated by $(2^i + 4)^3 - 8^i$, where i is the level in the local tree (not the "Level" shown in Table 3). For example, for level one in the local tree, the amount of cells will be $(2^1 + 4)^3 - 8^1$ which is equivalent to 26×8. This is why the "Bytes" is the same for the "Global M2L" and the first level of the "Local M2L" in Table 3.

Table 3: Statistics of the M2L communication.

(a) 128 Processes

Level	Cells	Sends	Bytes
0	1	0	0
1	8	0	0
2	64	26	46592
3	512	26	46592
4	4096	26	46592
5	32768	26	100352
6	262144	26	272384
7	2097152	26	874496

(b) 1024 Processes

Level	Cells	Sends	Bytes
0	1	0	0
1	8	0	0
2	64	26	46592
3	512	26	46592
4	4096	26	46592
5	32768	26	46592
6	262144	26	100352
7	2097152	26	272384
8	16777216	26	874496

(c) 8192 Processes

Level	Cells	Sends	Bytes
0	1	0	0
1	8	0	0
2	64	26	46592
3	512	26	46592
4	4096	26	46592
5	32768	26	46592
6	262144	26	46592
7	2097152	26	100352
8	16777216	26	272384
9	134217728	26	874496

6.3 Model Validation

We compare the actual communication time for the M2L communication with our performance model on Shaheen, Mira, Titan, and Piz Dora. We compare against same combination of models as in the multigrid study [11]. The combinations are:

1. Baseline model ($\alpha - \beta$ model)
2. With distance penalty ($\alpha - \beta - \gamma$ model)
3. With distance and bandwidth penalty (β penalty)
4. With distance and bandwidth penalty, plus multicore penalty on latency (α, β penalty)
5. With distance and bandwidth penalty, plus multicore penalty on distance (β, γ penalty)
6. With distance and bandwidth penalty, plus multicore penalty on latency and distance (α, β, γ penalty)

The results on Shaheen are shown in Figure 5. The actual measured performance is shown as a black line, where an error bar is drawn according to the standard deviation in communication time among the different MPI ranks. By comparing the Bytes in Table 3 with the communication time in Figure 5, we see that the deepest four levels that belong to the "Local M2L" phase have a communication time that is proportional to the data size being sent. The main discrepancy in the models is caused by the β penalty, for which the ratio between the theoretical injection bandwidth and the `b_eff` benchmark results is accounted for. The actual communication time agrees well with the models with α, β, and γ penalties.

For the shallow levels that belong to the "Global M2L" phase, the communication time increases as the level decreases/coarsens. Here, and in Figures 7, 8, and 9 to follow, the "Global M2L" levels are 3 in part (a), 3 and 4 in part (b), and 3, 4, and 5 in part (c). The reason for the increase can be understood by looking back at Figure 3, where the "Global M2L" is communicating with farther processes at coarser levels of the tree. Since we are mapping the geometric partitioning of the octree to the 3-D torus network of Shaheen, the proximity in the octree directly translates to the proximity in the network. Therefore, even though the data size is constant for all levels in the "Global M2L" phase, the number of hops is larger, which accounts for switching delays and also network contention to some extent. This increases the communication time at coarser levels and the models that incorporate γ are able to predict this behavior.

In Figure 6, the M2L communication time on Shaheen is plotted against the MPI rank to show the load balance between the processes. Each color shows M2L communication at a different level of the tree structure, and the numbers in the legend represent the levels. The communication time of each level is stacked on top of each other so that the total hight of the area

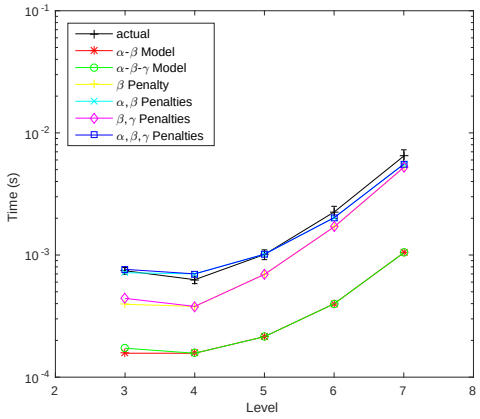

(a) 128 processes

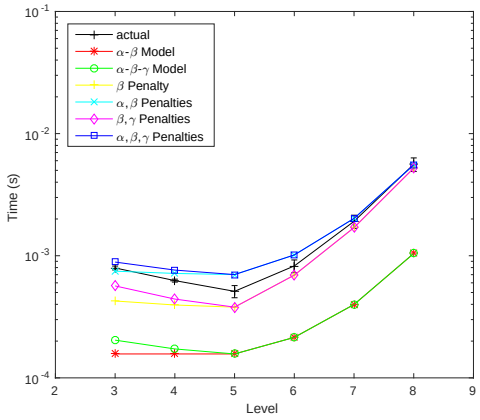

(b) 1024 processes

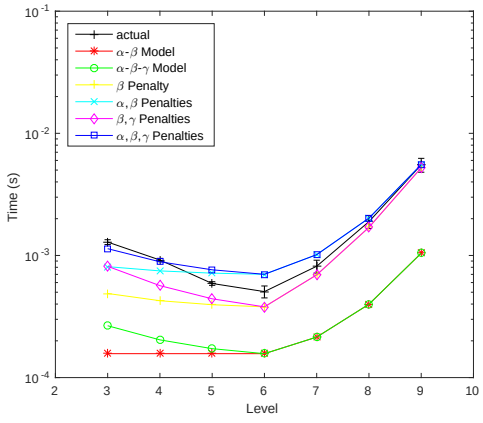

(c) 8192 processes

Figure 5: Performance model prediction and actual time for M2L communication phase on Shaheen.

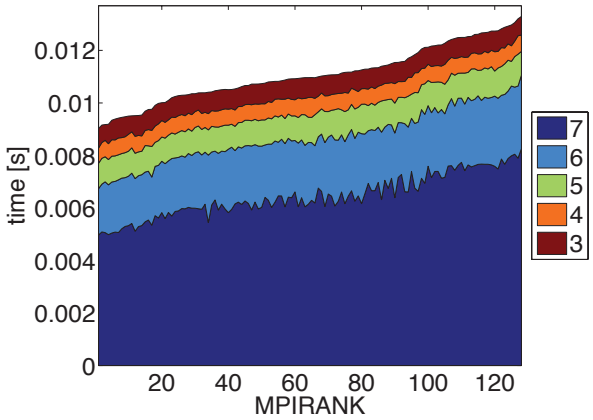

(a) 128 processes

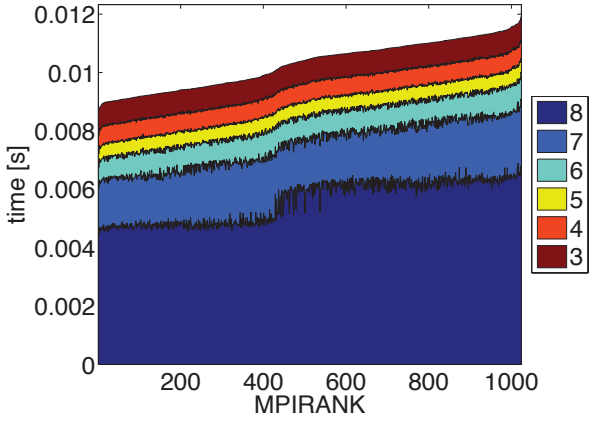

(b) 1024 processes

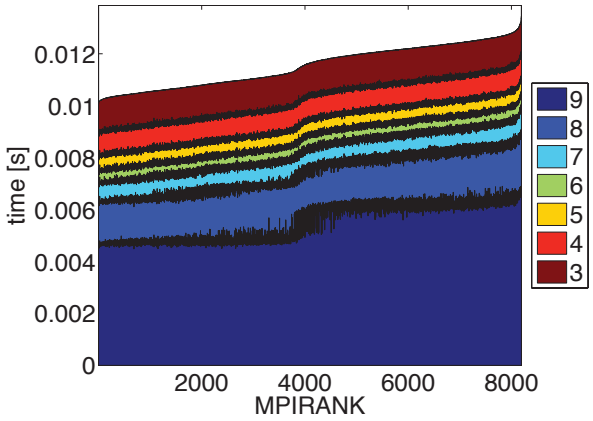

(c) 8192 processes

Figure 6: Load balance of M2L communication phase on Shaheen.

plot represents the total M2L communication time shown in Figure 5. The MPI ranks are sorted according to the total M2L communication time for better visibility in the small differences between processes. As can be seen from the figure, the load balance is quite good. The imbalance seems to come from the finest levels, which are 7, 8, and 9 for 128, 1024, and 8192 processes, respectively.

The M2L communication time on Mira is plotted along with the six model predictions in Figure 7. Similarly to the runs on Shaheen, the main difference in the model predictions is caused by the β penalty. We also see a discrepancy between the model predictions with and without the α penalty for the "Global M2L" phase (coarser levels). The multicore penalty is very small on the Bluegene/Q. This lack of multicore penalty has been observed in other applications where the use of hybrid OpenMP+MPI approach did not improve the performance over a flat MPI approach [21]. Contrary to the runs on Shaheen, the communication time has a nearly flat profile for the "Global M2L" phase. This is because the 5-D torus network minimizes the number of hops and network contention so the degradation at coarse levels of the tree is minimal. Far nodes in the octree are not so far in the Bluegene/Q network topology.

Figure 8 shows the M2L communication time on Titan along with the six model predictions. Similarly to the previous two cases, the difference between the model predictions is mainly due to the correction for the inverse bandwidth. This difference in the theoretical injection bandwidth and measured effective bandwidth seems to have the largest effect on all three architectures. What is different from the previous two cases is the large jump in the actual communication time for the "Global M2L" phase. For example, for the 8192 process run level 5 is taking about 10 times more than level 6 even though the message size is $46,592$ Bytes for both cases. The γ term in the current performance models anticipates such behavior. The error bars in the actual timings are quite large, which indicates that there is a large load imbalance compared to the previous two systems. The concave-convex switch at level 5 in 8(b) is not well predicted by the models, but the more refined models do pick it up at level 6 in 8(c). Though a good match between the measurements and simple models is not realized for M2L at all granularities on Titan, performance trends are generally well predicted.

The M2L communication time on Piz Dora is plotted along with the six model predictions in Figure 9. In the case of 128 processes, the best fitting model is the baseline model plus only the distance penalty. Increasing the number of processes increases the pos-

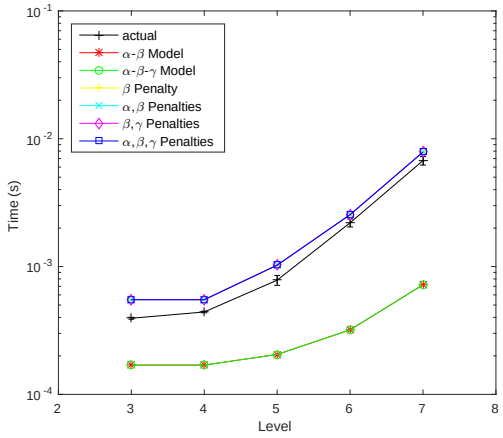

(a) 128 processes

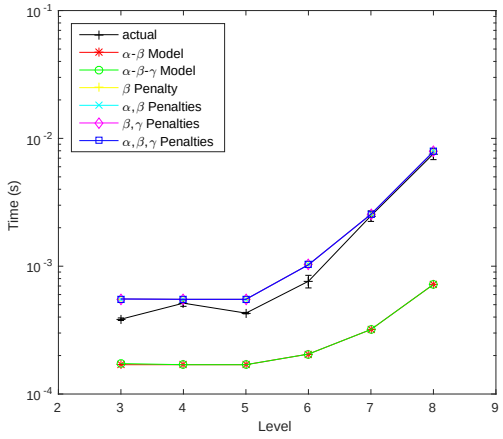

(b) 1024 processes

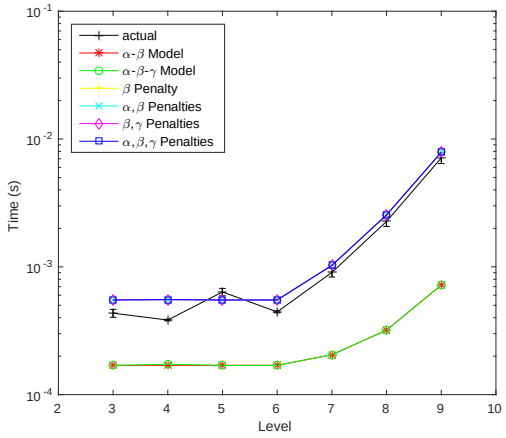

(c) 8192 processes

Figure 7: Performance model prediction and actual time for M2L communication phase on Mira.

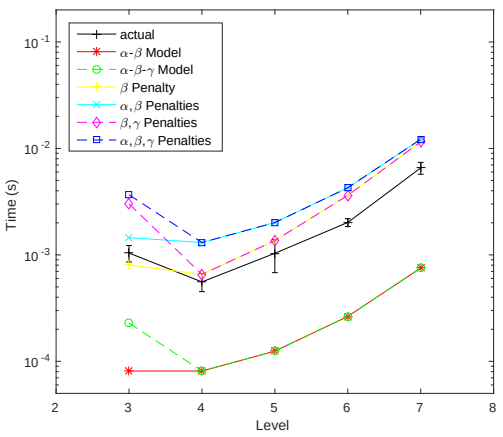

(a) 128 processes

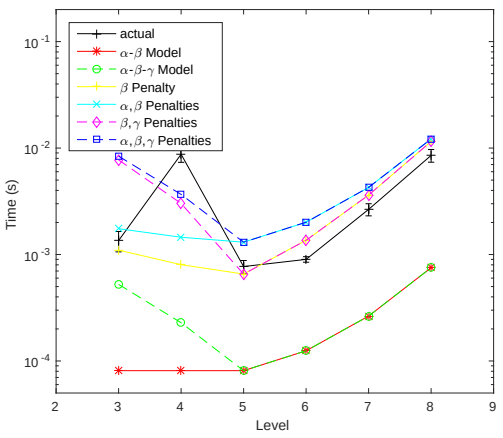

(b) 1024 processes

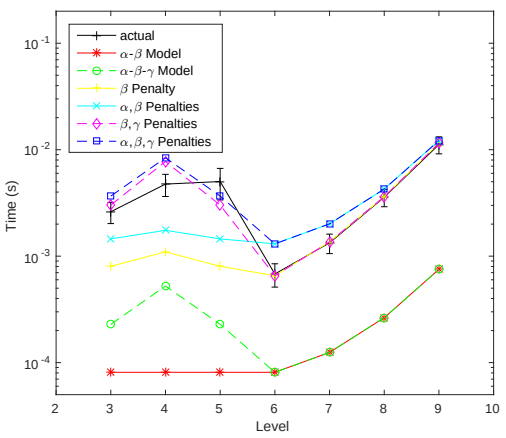

(c) 8192 processes

Figure 8: Performance model prediction and actual time for M2L communication phase on Titan.

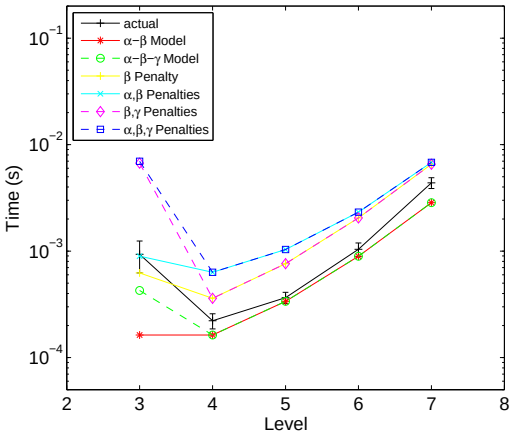

(a) 128 processes

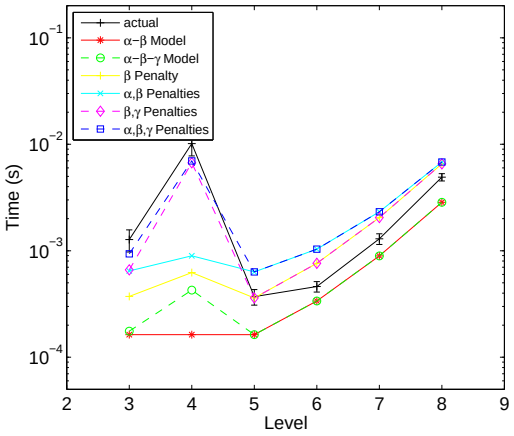

(b) 1024 processes

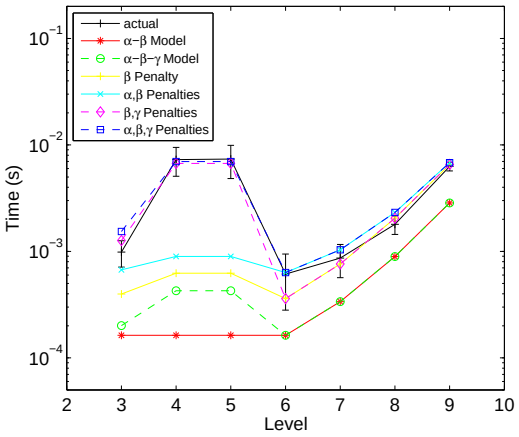

(c) 8192 processes

Figure 9: Performance model prediction and actual time for M2L communication phase on Piz Dora.

sibility of contention and makes the model with all penalties the best fitting model. Similar to the runs on Titan, there is a large jump in the actual communication time for the "Global M2L" phase with even worse load balancing suggested by the large error bars. The performance model is able to predict the poor performance at the coarse levels.

7 Conclusion

The goal of this work is to model the global communication of the FMM, to be able to anticipate challenges on future exascale machines. To improve model fidelity, we consider penalties based on machine constraints including distance effects, reduced per core bandwidth, and the number of cores per node. We observe a good match between the (α, β, γ) model with multicore penalties and the actual communication time. The discrepancy between the other models means that all components of the model; latency (α), bandwidth (β), hops (γ), and multicore penalty must be taken into account when predicting the communication performance of FMM.

In our benchmark tests, we compare the performance models with measurements for the M2L communication, since this is the dominant part of the FMM communication. Our observations are consistent with those of the studies by Gahvari et al. [11], where the performance of an algebraic multigrid method is analyzed using the same model. The measurements fall within the bounds of the performance models, and match best with the model where latency, bandwidth, hops, and multicore penalty are all taken into account.

The present communication model is able to predict the performance on four HPC systems possessing different characteristics. To our knowledge, this is the first formal characterization of inter-node communication in FMM, which validates the model against actual measurements of communication time. Furthermore, the FMM implementation considered in this paper has a provably best theoretical communication complexity among FMM algorithms [32], so demonstrations for other implementations may be less relevant in practice.

Our current FMM code does not support asynchronous data transfer so we are not able to provide a reference implementation for the performance model that includes asynchronous data transfers.

The ultimate communication model is predictive in an absolute sense; however, on complex systems, this objective is often out of reach, or of a difficulty out of proportion to its benefit when there exists a

simpler model that is inexpensive and sufficient to guide coding decisions leading to improved scaling. The current model provides such guidance.

Looking into the future, we will most likely be seeing more network topologies with larger diameter (more hops). Large radix networks seem to be the current trend, but with the exponential increase in the node count the increase of the network diameter is unavoidable. Our communication model with the distance penalty is able to capture the increase in communication time at the coarse levels of the FMM communication on Titan's torus network. This should allow predicting the communication bottlenecks on future networks with larger diameter.

The performance model herein is applicable to evolving heterogeneous systems, such as GPUs or Xeon Phis. This is because the accelerators and coprocessors affect the per-node computation but not the inter-node communication. Nor is the model affected by the on-node computational performance of FMM, as long as the accelerators and coprocessors are not using more than one MPI process, which is the optimal way to use the current generation of such hardware.

Acknowledgements

We acknowledge system access and the generous assistance of the staffs at four facilities for the performance tests herein: the KAUST Supercomputing Laboratory; the Argonne Leadership Computing Facility at Argonne National Laboratory, which is supported by the Office of Science of the U.S. Department of Energy under contract DE-AC02-06CH11357; the Oak Ridge Leadership Computing Facility at Oak Ridge National Laboratory, which is supported by the Office of Science of the U.S. Department of Energy under Contract No. DE-AC05-00OR22725; and the Swiss National Supercomputing Centre (CSCS), under project ID g81.

Author Biographies

Huda Ibeid received her BSc degree in Computer Engineering from the University of Jordan and is currently a PhD candidate in Computer Science at the King Abdullah University of science and Technology (KAUST). Her research interests include fast algorithms for particle-based simulations, fast algorithms on parallel computers and GPUs, design of parallel numerical algorithms, parallel programming models and performance optimizations for heterogeneous GPU-based systems.

Rio Yokota obtained his PhD from Keio University, Japan, in 2009 and worked as a postdoctoral researcher with Prof. Lorena Barba at the University of Bristol and then Boston University. He has worked on the implementation of fast N-body algorithms on special-purpose machines such as MDGRAPE-3, and then on GPUs after CUDA was released, and on vortex methods for fluids simulation. He joined the King Abdullah University of Science and Technology (KAUST) as a research scientist, where he continued to work on fast multipole methods. He is now at the Tokyo Institute of Technology as an Associate Professor.

David Keyes is the director of the Extreme Computing Research Center at KAUST and an Adjoint Professor of Applied Mathematics at Columbia University. Keyes graduated in Aerospace and Mechanical Sciences from Princeton University and earned a doctorate in Applied Mathematics from Harvard University. He did postdoctoral work in the Computer Science Department of Yale University. He works at the algorithmic interface between parallel computing and the numerical analysis of partial differential equations, across a spectrum of aerodynamic, geophysical, and chemically reacting flows.

References

[1] J. Barnes and P. Hut. O($N \log N$) force-calculation algorithm. *Nature*, 324:446–449, 1986.

[2] R. Beatson and L. Greengard. A short course on fast multipole methods. In *Wavelets, Multilevel Methods and Elliptic PDEs*, pages 1–37. Oxford Science Publications, 1997.

[3] A. Chandramowlishwaran, K. Madduri, and R. Vuduc. Diagnosis, tuning, and redesign for multicore performance: A case study of the fast multipole method. In *SC '10 Proceedings of the 2010 ACM/IEEE International Conference for High Performance Computing, Networking, Storage and Analysis*, 2010.

[4] A. Chandramowlishwaran, S. Williams, L. Oliker, I. Lashuk, G. Biros, and R. Vuduc. Optimizing and tuning the fast multipole method for state-of-the-art multicore architectures. In *Proceeding of the International Parallel Distributed Processing Symposium (IPDPS)*, pages 1–12, 2010.

[5] H. Cheng, L. Greengard, and V. Rokhlin. A fast adaptive multipole algorithmin three dimensions. *Journal of Computational Physics*, 155(2):468–498, 1999.

[6] M. J. Clement and M. J. Quinn. Symbolic performance prediction of scalable parallel programs. In

Proceedings of the International Parallel Processing Symposium, pages 635–639, April 1995.

[7] L. DeRose and D. A. Reed. SvPablo: A multi-language, architecture-independent performance analysis system. In *Proceeding of the International Conference on Parallel Processing*, pages 311–318, Augest 1999.

[8] J. Dongarra and F. Sullivan. Guest Editors Introduction to The Top 10 Algorithms. *Computing in Science and Engineering*, 2:22–23, 2000.

[9] I. Foster. *Designing and Building Parallel Programs*. Addison-Wesley, 1995.

[10] I. T. Foster and P. H. Worley. Parallel algorithms for the spectral transform method. *SIAM Journal on Scientific and Statistical Computing*, 18(3):806–837, 1997.

[11] H. Gahvari, A. H. Baker, M. Schulz, U. M. Yang, K. E. Jordan, and W. Gropp. Modeling the performance of an algebraic multigrid cycle on HPC platforms. In *ICS '11 Proceedings of the International Conference on Supercomputing*, pages 172–181, 2011.

[12] H. Gahvari, W. Gropp, K. E. Jordan, M. Schulz, and U. M. Yang. Algebraic multigrid on a dragonfly network: First experience on a Cray XC30. In *Proceeding of the 5th International Workshop on Performance Modeling, Benchmarking and Simulation of High Performance Computer Systems (PMBS14)*, November 2014.

[13] N. L. Gorn and D. V. Berkov. Adaptation and performance of the fast multipole method for dipolar systems. *Journal of Magnetism and Magnetic Materials*, 272-276:698–700, 2004.

[14] L. Greengard, M. C. Kropinski, and A. Mayo. Integral equation methods for Stokes flow and isotropic elasticity in the plane. *Journal of Computational Physics*, 125:403–414, 1996.

[15] L. Greengard and V. Rokhlin. A fast algorithm for particle simulations. *Journal of Computational Physics*, 73(2):325–348, 1987.

[16] L. Greengard and Rokhlin V. On the efficient implementation of the fast multipole algorithm. Research Report RR-602, Yale University, 1988.

[17] W. D. Gropp, D.K. Kaushik, D.E. Keyes, and B.F. Smith. Toward realistic performance bounds for implicit CFD codes. In *Proceedings of Parallel CFD'99*, pages 23–26, May 1999.

[18] P. Jetley, L. Wesolowski, F. Gioachin, L. V. Kale, and T. R. Quinn. Scaling hierarchical N-body simulations on GPU clusters. In *SC '10 Proceedings of the 2010 ACM/IEEE International Conference for High Performance Computing, Networking, Storage and Analysis*, pages 1–11, 2010.

[19] D. Kerbyson, H. Alme, A. Hoisie, F. Petrini, A. Wasserman, and M. Gittings. Predictive performance and scalability modeling of a large-scale application. In *Proceedings of the 2001 ACM/IEEE conference on Supercomputing*, pages 1–12, 2001.

[20] I. Lashuk, A. Chandramowlishwaran, H. Langston, T.-A. Nguyen, R. Sampath, A. Shringarpure, R. Vuduc, L. Ying, D. Zorin, and G. Biros. A massively parallel adaptive fast multipole method on heterogeneous architectures. In *Proceedings of the Conference on High Performance Computing Networking, Storage and Analysis*, pages 1–12, 2009.

[21] M. Lee, N. Malaya, and R. D. Moser. Petascale direct numerical simulation of turbulent channel flow on up to 768k cores. In *Proceedings of the Conference on High Performance Computing Networking, Storage and Analysis*, Denver, CO, USA, Novermber 16-22 2013.

[22] P. Luszczek and J. Dongarra. Introduction to the HPC Challenge Benchmark Suite. Technical Report ICL-UT-05-01, University of Tennessee, Knoxville, March 2005.

[23] C. L. Mendes. *Performance Scalability Prediction on Multicomputers*. PhD thesis, University of Illinois, Urbana-Champaign, May 1997.

[24] C. L. Mendes and D. A. Reed. Integrated compilation and scalability analysis for parallel systems. *International Conference on Parallel Architectures and Compilation Techniques (PACT'98)*, pages 385– 392, October 1998.

[25] J. M. Perez-Jorda and W. Yang. On the scaling of multipole methods for particle-paticle interactions. *Chemical Physics Letters*, 282:71–78, 1998.

[26] W. T. Rankin. *Efficient Parallel Implementations of Multipole Based N-body Algorithm*. PhD thesis, Duke University, 1999.

[27] A. Snavely, N. Wolter, and L. Carrington. Modeling application performance by convolving machine signatures with application profiles. In *Proceeding of the IEEE Workshop on Workload Characterization*, pages 149–156, December 2001.

[28] B. Van de Wiele, F. Olyslager, and L. Dupre. Application of the fast multipole method for the evaluation of magneto-static fields in micromagnetic computations. *Journal of Computational Physics*, 227:9913–9932, 2008.

[29] W. R. Wolf and S. K. Lele. Aeroacoustic integrals accelerated by fast multipole method. *AIAA Journal*, 49(7):1466–1477, 2011.

[30] P. H. Worley. Performance evaluation of the IBM SP and the Compaq AlphaServer SC. In *Proceeding of the ACM International Conference of Supercomputing 2000*, pages 235–244, 2000.

[31] R. Yokota, J. Pestana, H. Ibeid, and D. E. Keyes. Fast multipole preconditioners for sparse matrices arising from elliptic equations. *arXiv:1308.3339v2*, 2014.

[32] R. Yokota, G. Turkiyyah, and D. Keyes. Communication complexity of the fast multipole method and its algebraic variants. *Supercomputing Frontiers and Innovations*, 1(1):63–84, 2014.

[33] J.-S. Zhao and W.-C. Chew. Three-dimensional multilevel fast multipole algorithm from static to electrodynamic. *Microwave and Optical Technology Letters*, 26(1):43–48, 2000.